PERGAMON

Chemical Engineering Science 58 (2003) 3233–3241

Chemical Engineering Science

www.elsevier.com/locate/ces

Interpreting the effects of operating variables on the induction period of $CaCl_2$–Na_2CO_3 system by a cluster coagulation model

C. Y. Tai*, W. C. Chien

Department of Chemical Engineering, National Taiwan University, No 1, Sec 4, Roosevelt Road, Taipei 10617, Taiwan

Received 1 April 2002; received in revised form 21 August 2002; accepted 12 March 2003

Abstract

In this article the effects of several operating variables, including supersaturation, temperature, and the presence of additive and seeds on the induction period of $CaCO_3$ were studied experimentally and theoretically. In experimental, the induction period was measured by a conductivity method so that the induction period was well identified. The results show that the induction period increases with decreasing supersaturation and temperature. The presence of Mg^{2+} in solution prolongs the induction period and the addition of seeds reduces the induction period. In theoretical, a cluster coagulation model, which brings together the current nucleation models and the theories describing the behavior of colloidal suspensions, was applied to estimate the induction period under various operating variables. A comparison between the two results shows that the present model is a suitable one to interpret the effects of various operating variables on the induction period of aqueous $CaCl_2$–Na_2CO_3 solution.

Keywords: Coagulation; Crystallization; Nucleation; Precipitation; Calcium carbonate; Induction period

1. Introduction

The induction period, t_{ind}, is defined as the time interval between the creation of supersaturation, S_a, and the formation of critical nuclei. Many experimental methods have applied to determine the induction period such as conductivity method (Söhnel & Mullin, 1978, 1982), intensity of transmitted or scattered light method (Wakita & Masuda, 1983; Carosso & Pelizzetti, 1984; Kibalczyc & Bondarczuk, 1985), heat released method (Glasner & Tassa, 1972; Kibalczyc & Zielenkiewicz, 1987), activity of precipitated ions method (Verdoes, Kashchiev, & van Rosmalen, 1992) and pH method (Gómez-Morales, Torrent-Burgués, & Rodríguez-Clemente, 1996). These previous investigations show that the induction period is influenced by several important factorssuch as supersaturation (Söhnel & Mullin, 1982), temperature (Mullin & Žáček, 1981), presence of impurity (Söhnel & Mullin, 1982; Pokrovsky, 1998), addition of seeds (Verdoes et al., 1992), and so on. Among these factors supersaturation is the most important factor to affect the induction period, which increases with decreasing supersaturation. Conventionally, two ways are used to interpret the experimental t_{ind}-S_a data. One of them is the empirical method that predicted a linear relationship between $\log t_{ind}$ and $\log S_a$ (Söhnel & Garside, 1992). According to this method, the empirical nucleation rate constant and nucleation order can be estimated from the intercept and slope of a straight line, respectively. The second one is based on the classical nucleation theory that predicted a linear relationship between $\log t_{ind}$ and $(\log S_a)^{-2}$. According to this theoretical analysis, Söhnel and Mullin (1988) inferred that the change in surface tension at different supersaturation range accounted for the switch of nucleation mechanism at a certain S_a. Recently, Chien, Tai, and Hsu (1999) applied a cluster coagulation model to calculate the induction period at different levels of supersaturation, yet a linear relationship between $\log t_{ind}$ and $(\log S_a)^{-2}$ did not exist.

Another factor that has an important influence on the induction period is the temperature, T. In most investigating cases the induction period decreases with increasing temperature. Conventionally, the effect of temperature on induction period was interpreted by the classical nucleation theory, which predicts a linear relationship between $\log t_{ind}$

* Corresponding author. Tel.: +886-223620832; fax: +886-2-2362-3040.
E-mail address: cytai@ccms.ntu.edu.tw (C. Y. Tai).

0009-2509/03/$ - see front matter © 2003 Elsevier Ltd. All rights reserved.
doi:10.1016/S0009-2509(03)00184-2

and $(T^3 \log S_a^2)^{-1}$ (Mullin & Žáček, 1981; Mullin, 1993). For each temperature a different straight line is obtained, and the slope of the straight line allows a value of interfacial tension, δ, to be calculated. The values of interfacial tension so determined are therefore temperature-dependent and they decreases with increasing temperature. Based on the analysis the decrease in induction period at higher solution temperature is mainly caused by a decrease in the interfacial tension. For example, in the study of Mullin and Žáček (1981) by keeping the supersaturation constant ($S_a = 1.5$), the induction period of potash alum decreases from 200 s at $T = 288$ K with $\delta = 3.14$ mJ/m^2 to 25 s at $T = 308$ K with $\delta = 2.03$ mJ/m^2. The presence of impurities in a system can affect the induction period considerably, but it is virtually impossible to predict. Some of the impurities increase the induction period, whereas others may cause a decrease of it or have no effect. The effects of impurities are generally interpreted by a change of equilibrium solubility or the solution structure, by adsorption or chemisorption on nuclei or heteronuclei, and by chemical reaction or complex formation in the solution (Mullin, 1993). Söhnel and Mullin (1982) studied the precipitation of $CaCO_3$ formed by mixing equimolar solutions of $CaCl_2$ and Na_2CO_3 at 298 K. They found that anions Br^-, NO_3^-, Cl^- and F^- exert little influence on t_{ind}. The cations K^+, Cr^{3+} and Ni^+ are similarly inactive, only Mn^{2+} and Mg^{2+} lengthen the induction period. They concluded that the increase in t_{ind} caused by the presence of impurity is due to an increase in the crystal-solution interfacial tension. Recently, Pokrovsky (1998) also found that the induction period of $CaCO_3$ increases with increasing Mg^{2+}/Ca^{2+} activity ratio in solution. The increase in t_{ind} is due to an increase in the crystal-solution interfacial tension at higher Mg^{2+}/Ca^{2+} region and due to an increase in the activity of Mg^{2+} at lower Mg^{2+}/Ca^{2+} region.

The addition of seed in solution usually decreases the induction period when comparing with the unseeded case at the same supersaturation. Verdoes et al. (1992) analyzed the induction period data collected from both unseeded and seeded precipitation experiments of $BaSO_4$ and $CaCO_3$. The analysis revealed some information on nucleation and growth mechanisms. However, their analysis is based on the classical nucleation theory, neglecting the interaction forces between the clusters and seeds. Recently, Qian and Botsaris (1997) presented a new mechanism of nuclei formation to explain the catastrophic secondary nucleation of potassium chloride solutions. They showed that the interparticle forces between embryos and embryos-crystal seeds were too important to be neglected in a suspension crystallizer.

In the present paper, the effects of supersaturation, temperature and presence of additive and seed crystals on the induction period are investigated experimentally and theoretically for the precipitation of $CaCO_3$. Experimentally, the induction period is estimated from the behavior of the temporal variation of a desupersaturated curve, which is a plot of solution conductivity against time. Some of the experimental results including temperature, presence of additives and seed crystals on the induction period have been presented (Tai & Chien, 2001). However, the experimental results were not interpreted by a theoretical model. Theoretically, the induction period is calculated by a cluster coagulation theory, which brings together the current nucleation models and the theories describing the behavior of colloidal suspensions. Finally, a comparison of induction period is made between experimental data and theoretical results.

2. Theoretical

The classical theory of homogeneous nucleation indicated that when the solution is supersaturated the monomers in solution start to coagulate and form clusters. If the size of a cluster exceeds a critical size, a nucleus forms and the subsequent growth of nucleus leads to a crystal. When the nucleation rate attains a steady state instantaneously, i.e., the transient period can be neglected, the time interval between the onset of supersaturation and the formation of a cluster of critical size is defined as the induction period, t_{ind}. It has been shown that the transient period is not important in the aqueous solutions of moderate supersaturation and viscosity (Nielsen, 1964; Söhnel & Mullin, 1988). In certain special cases; however, at very low supersaturation or very high viscosity the transient period cannot be ignored (Nielsen, 1964; Packter, 1974). Meanwhile, Kubota, Kawakami, and Tadaki (1986) have suggested a method for taking into account the transient period.

The temporal variation of cluster size distribution can be described by the classic Smoluchowski theory of coagulation (Sonntag & Strenge, 1987). However, since the rate constants for the coagulation between clusters of various sizes and the corresponding mechanism are both unknowns, evaluation of the cluster size distribution becomes nontrivial. This problem is circumvented by considering the mean or averaged behavior of the system. It was assumed that only the $\bar{g}$-mers are present initially, and they coagulate to form $2\bar{g}$-mers. Then the $2\bar{g}$-mers coagulate to give $4\bar{g}$-mers, and so on, until the critical nuclei, i.e., g_c-mers, are formed. According to this simplified model, the t_{ind} can be evaluated by the following correlation composed of three important terms related to diffusivity, coagulation concentration, and critical nuclei size (Qian & Botsaris, 1997)

$$t_{ind} = \left(\frac{1}{8\pi D r_{\bar{g}}}\right)\left(\frac{1}{n_{\bar{g}}}\right)\left(\frac{g_c}{\bar{g}} - 1\right). \quad (1)$$

Substituting $D = kT/6\pi\eta r_{\bar{g}}$ (Sonntag & Strenge, 1987) into Eq. (1), we obtain

$$t_{ind} = \left(\frac{3\eta}{4kT}\right)\left(\frac{1}{n_{\bar{g}}}\right)\left(\frac{g_c}{\bar{g}} - 1\right). \quad (2)$$

In these expression, D is the diffusivity of clusters, $\bar{g}$ is the dominating size of clusters, $r_{\bar{g}}$ is the radius of $\bar{g}$-mer, $n_{\bar{g}}$ is the number concentrations of $\bar{g}$-mer, η is the viscosity of the liquid phase, k is the Boltzmann constant, and T is the

absolute temperature. The critical cluster size can be derived from the classical nucleation theory and expressed as

$$g_c = \frac{32\pi V_m^2 \delta^3}{3(kT \ln S_a)^3} \tag{3}$$

and $n_{\bar{g}}$ can be evaluated by

$$n_{\bar{g}} = n_1 \exp\left(-\frac{\Delta G_{\bar{g}}}{kT}\right) \tag{4}$$

where

$$\Delta G_{\bar{g}} = (4\pi)^{1/3}\delta(3\bar{g}V_m)^{2/3} - \bar{g}(kT \ln S_a) \tag{5}$$

and

$$n_1 = \frac{n_0}{\sum_{\bar{g}=1}^{g_c} g(n_{\bar{g}}/n_1)} \tag{6}$$

Here n_1 is the number concentration of monomer, which can be calculate by the initial concentration of monomer, n_0, and Eqs. (4) and (5), $\Delta G_{\bar{g}}$ is the total excess free energy for the formation of a $\bar{g}$-mer, δ and V_m are the interfacial tension of the crystal and the volume of a monomer respectively. The supersaturation can be evaluated by

$$S_a = \frac{C_{CaCO_3}\gamma_{\pm}}{C_{CaCO_{3eq}}\gamma_{\pm eq}}, \tag{7}$$

where C_{CaCO_3} is the initial concentration of $CaCO_3$, $C_{CaCO_{3eq}}$ is the equilibrium concentration of $CaCO_3$ in an aqueous NaCl solution which can be found in the literature (Söhnel & Garside, 1992), $\gamma_{\pm}$ and $\gamma_{\pm eq}$ are the mean activity coefficient and equilibrium mean activity coefficient respectively, which can be estimated from Bromley correlation (Bromley, 1973). Substituting Eqs. (3)–(6) into Eq. (2) gives

$$t_{ind} = \left\{\frac{3\eta}{4kT}\right\}\left\{n_1^{-1}\exp\left[-\bar{g}\ln S_a + \frac{\delta}{kT}(4\pi)^{1/3}(3\bar{g}V_m)^{2/3}\right]\right\} \times \left\{\frac{32\pi V_m^2\delta^3}{3\bar{g}(kT\ln S_a)^3} - 1\right\}. \tag{8}$$

In Eq. (8) the three main terms, which are related to diffusivity, coagulation concentration, and critical nuclei size, are separated by braces, { }.

When the seed crystal is introduced into the supersaturated solution, the clusters are attracted by the van der Waals field of the seed crystal. Considering the van der Waals attractive energy between the cluster and seed crystal, the concentration of $\bar{g}$-mer at a distance d from the crystal surface, $n'_{\bar{g}}$, relative to its concentration in the bulk solution, $n_{\bar{g}}$, is given by (Qian & Botsaris, 1997)

$$n'_{\bar{g}} = n_{\bar{g}} \exp\left(\frac{A}{6kT}\frac{r_1}{d}\bar{g}^{1/3}\right), \tag{9}$$

where A is the Hamaker constant, which value is about 1.61×10^{-20} J for $CaCO_3$ in water (Bergström, 1997), and r_1 is the radius of a spherical monomer. Replacing $n_{\bar{g}}$ with $n'_{\bar{g}}$ in Eq. (2), the induction period of seeded solution, $t_{ind,s}$, can be expressed as

$$t_{ind,s} = \left(\frac{3\eta}{4kT}\right)\left(\frac{1}{n'_{\bar{g}}}\right)\left(\frac{g_c}{\bar{g}} - 1\right). \tag{10}$$

Substituting Eqs. (3)–(6) and Eq. (9) into Eq. (10) gives

$$t_{ind,s} = \left\{\frac{3\eta}{4kT}\right\}\left\{n_1^{-1}\exp\left[-\bar{g}\ln S_a + \frac{\delta}{kT}(4\pi)^{1/3}(3\bar{g}V_m)^{2/3} - \frac{A}{6kT}\frac{r_1}{d}\bar{g}^{1/3}\right]\right\} \times \left\{\frac{32\pi V_m^2\delta^3}{3\bar{g}(kT\ln S_a)^3} - 1\right\}. \tag{11}$$

Eq. (8) is used in the unseeded case for investigating the effects of supersaturation, temperature and impurities on the induction period. On the other hand, Eq. (11), which involves one more parameter d, is used to calculate the induction period of $CaCO_3$ when seed crystals are present in the aqueous solution of $CaCl_2$–Na_2CO_3.

3. Experimental

The experimental apparatus, which consists mainly of three parts, i.e., a reagent feeding system, a crystallizer with temperature control, and a data acquisition system, has been reported in a previous study (Chien et al., 1999). Chemicals of guaranteed grade calcium carbonate, extra-pure grade anhydrous sodium carbonate, and extra-pure magnesium chloride hexahydrate purchased from Nacalai Tesque Co., and high quality water with a specific resistivity 18 MΩ-cm was used. The water was filtered through a 0.2 μm filter before use.

The experimental procedures are described briefly below. A desired quantity of water and 0.1 M $CaCl_2$ solutions were poured into the crystallizer and mixed by a magnetic stirrer to form a solution of specified concentration. After the solution temperature became steady at 298 K and the conductivity remained constant for several minutes, a required quantity of 0.1 M Na_2CO_3 solution at 298 K was added into the crystallizer. The solution conductivity increased rapidly to a higher level and stayed there for a certain period of time once the mixing is complete. Then, a decrease in conductivity was observed while the solution was still clear. Afterwards, the solution became turbid as detected by naked eyes. The experiment was stopped after the conductivity had no more significant change. After each run, the experimental apparatus was rinsed with 0.1 M aqueous HCl solution to remove residual precipitate.

In the case for investigating additive effect, the procedures are the same except that a desired quantity of 0.1 M

aqueous $MgCl_2$ solution was added into the solution of crystallizer before the addition of 0.1 M aqueous Na_2CO_3 solution. In all runs, the solution temperature is kept at 298 K. The concentrations of magnesium ion investigated in the present work ranges from 0.0003 to 0.0040 kgmol/m^3.

In the case of seeded experiment, the procedure differs only in having the seed crystals placed in the solution. The seed crystals with a size of 355–425 μm and total weight of 0.12 ± 0.01 g were added into the solution before adding the 0.1 M aqueous Na_2CO_3 solution.

4. Results and discussion

In this study factors that affect the induction period of $CaCO_3$ formed by mixing equalmolar solutions of $CaCl_2$ and Na_2CO_3 are investigated, including supersaturation, temperature, and addition of additive and seed crystals. To determine t_{ind} experimentally, typical desupersaturated curves represented by curve (a) for 288 K and curve (b) for 308 K are shown in Fig. 1. The t_{ind} is identified by the change of conductivity as shown in Fig. 2, which is an enlarged figure of the part for time interval between 0 and 250 s shown in Fig. 1. The experimental errors of t_{ind}-data obtained in the present work are about ±15% for various operating conditions. The result of unseeded case at 25°C is shown in Fig. 3. On the other hand, to calculate the induction period from Eq. (8) for unseeded case and Eq. (11) for seeded case, the following values are used; $\eta = 0.001$ Pa s, $k = 1.38 \times 10^{-23}$ J/K, and $V_m = 6.13 \times 10^{-29}$ m^3/molecule, which is calculated from $M_w/\rho N_A$, using $M_w = 0.1$ kg/mol, $\rho = 2710$ kg/m^3 and $N_A = 6.02 \times 10^{23}$ molecules/mol. Besides, the most proper values of $\bar{g}$ and δ are estimated by fitting the experimental data of induction period.

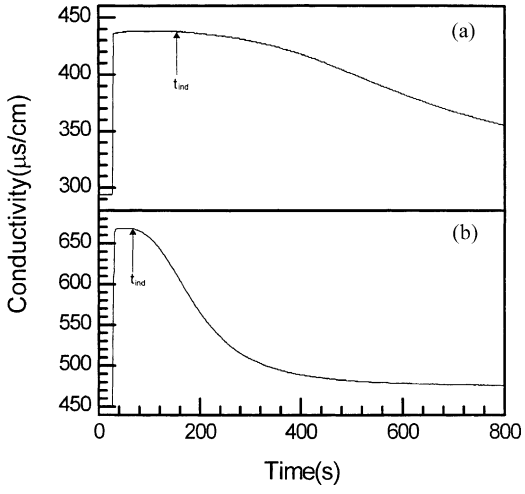

Fig. 1. Typical desupersaturation curves at $[CaCl_2] = [Na_2CO_3] = 0.0025$ kgmol/m^3 for different operating temperatures. (a) $T = 288$ K. (b) $T = 308$ K.

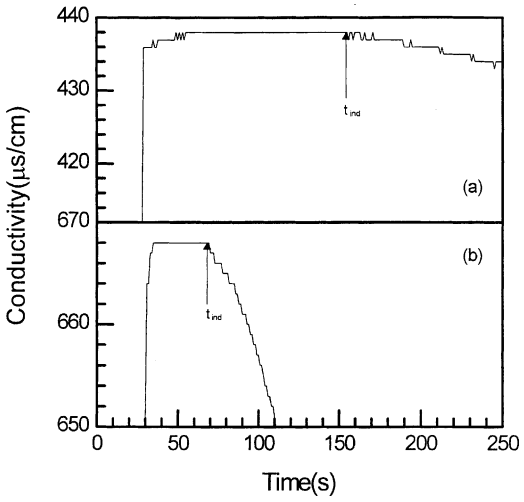

Fig. 2. Enlarged conductivity-time curves showing t_{ind} for two temperature levels. (a) $T = 288$ K. (b) $T = 308$ K.

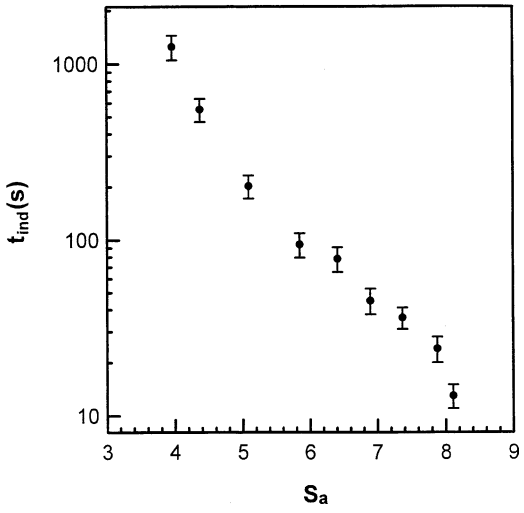

Fig. 3. The experimental errors of unseeded t_{ind} data at 25°C.

4.1. Effect of supersaturation on induction period

Fig. 4 illustrates the experimental data of induction period obtained for various supersaturations, and the theoretical curves calculated from Eq. (8) using assumed parameters $\bar{g}$ and δ for various supersaturation in the range 3 to 9. Both of the experimental and theoretical results show that the induction period decreases with increasing supersaturation at constant temperature. Comparing the experimental data with theoretical curves of induction period, it is found that the theoretical curve obtained at $\bar{g} = 2$ and $\delta = 68.4$ mJ/m^2 are most close to the experimental points. Choosing the best values for $\bar{g}$ and δ is based on the total absolute deviation, ε, between the theoretical and experimental induction periods. The ε is defined as $\sum |t_{ind,exp} - t_{ind,the}|/t_{ind,exp}$. The values of calculated ε for various $\bar{g}$ and δ are listed in Table 1. The first three values of ε show that 2 is a suitable

Table 1
A comparison of the calculated ε for various $\bar{g}$ and δ at 298 K ($\varepsilon = \sum |t_{\mathrm{ind,exp}} - t_{\mathrm{ind,the}}|/t_{\mathrm{ind,exp}}$)

	$t_{\mathrm{ind,\ the}}$ (S)								
S_a (dimensionless)	$t_{\mathrm{ind,exp}}$ (s)	$\bar{g}=1$, $\delta=70$	$\bar{g}=2$, $\delta=70$	$\bar{g}=3$, $\delta=70$	$\bar{g}=2$, $\delta=60$	$\bar{g}=2$, $\delta=68.3$	$\bar{g}=2$, $\delta=68.4$	$\bar{g}=2$, $\delta=68.5$	$\bar{g}=2$, $\delta=80$
3.96	1250	9.56E − 05	1998	182746	68.8	1132	1171	1211	54388
4.37	550	5.82E − 05	998	82640	34.3	566	585	605	27186
5.06	202	2.88E − 05	364	25812	12.5	206	213	220	9920
5.79	94	1.69E − 05	161	9910	5.51	91	94	97	4392
6.41	78	1.16E − 05	92.0	5156	3.14	52	54	56	2510
6.90	45	8.58E − 06	59.0	3054	2.01	33	34	35	1604
7.37	36	6.65E − 06	40.0	1935	1.35	22	23	24	1088
7.88	24	5.26E − 06	27.5	1249	0.93	16	16	17	753
8.41	13	4.75E − 06	23.4	1033	0.08	13	13	14	641
ε=		9.00	4.48	840	8.59	1.50	1.43	1.46	359

Note: δ in mJ/m^2

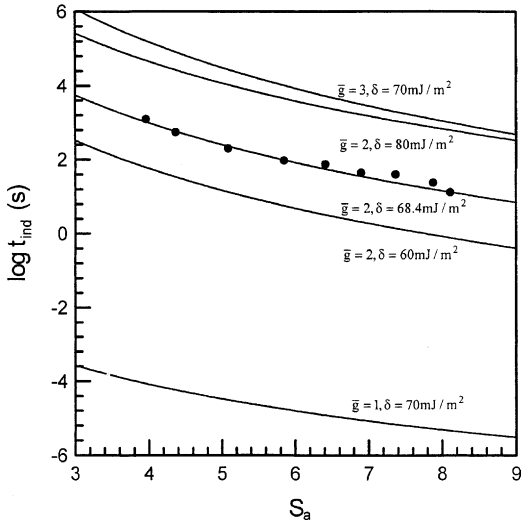

Fig. 4. Induction period as a function of supersaturation for different combination of $\bar{g}$-mers and interfacial tensions at 298 K: • experimental data; — theoretical curves of Eq. (8) by using the fitted parameters $\bar{g}$ and δ for various supersaturation in the range of $S_a = 3$ to 9.

value for $\bar{g}$. Further trial of δ values gives the smallest value of ε for $\delta = 68.4$ mJ/m^2. Therefore, the theoretical curve plotted by the parameters $\bar{g} = 2$ and $\delta = 68.4$ mJ/m^2 are most close to the experimental points as shown in Fig. 4. In general, the interfacial tension δ of $CaCO_3$ is assumed to be independent of supersaturation for a narrow range of supersaturation in the literature, i.e., 67.6 mJ/m^2 for $S_a = 8$–25 (Pokrovsky, 1998), 80 mJ/m^2 for $S_a = 20$–50 or 60 mJ/m^2 for $S_a = 10$–20 (Mullin, 1993), and 68 mJ/m^2 for $S_a = 14$–23 (Koutsoukos & Kontoyannis, 1984). Therefore, the value of $\delta = 68.4$ mJ/m^2 for $S_a = 3$–9 estimated from the present analysis is quite reasonable. For $\bar{g} = 2$, $\delta = 68.4$ mJ/m^2 and $T = 298$ K, the induction periods calculated from Eq. (8) for various supersaturations are summarized in Table 2. It can be seen that the theoretical values of t_{ind} are close to those obtained experimentally. The values of column 3, 4, and 5 represent the three terms appeared on the right-hand side of Eq. (8). Table 2 shows that the value of diffusivity term, $3\eta/4kT$, is a function of viscosity and temperature and thus independent of supersaturation. Here the viscosity of solution in the supersaturation range investigated is assumed to be constant because of the low solubility of sparingly soluble compounds. On the other hand, the inverse values of coagulation concentration term, $1/n_{\bar{g}}$, and the critical size term, $(g_c/\bar{g}) - 1$, decrease with increasing supersaturation. Therefore, according to the present theoretical analysis, the decrease in induction period at higher supersaturation is mainly caused by the higher coagulation concentration of clusters and the smaller critical nuclei size.

Conventionally, a plot of the logarithm of t_{ind} and the logarithm of S_a will yield a straight line expressed as (Söhnel & Garside, 1992)

$$\log t_{\mathrm{ind}} = k_1 - n \log S_a. \tag{12}$$

In Eq. (12) the slope of the line, n, reflects the order of nucleation process over a narrower range of supersaturation. Fig. 5 shows that the measured data of induction period and supersaturation follow the linear dependence of Eq. (12). The calculated value of n is 5.10 for $S_a = 3.96$–8.11, which is close to 4.79 for $S_a = 8$–25 reported by Pokrovsky (1998) for the unseeded precipitation of calcium carbonate. In his studies the end of induction period was determined by monitoring the pH drop or by measuring solution turbidity with a spectrophotometer.

4.2. Effect of temperature on induction period

Fig. 6 shows that the experimental and theoretical induction period as a function of supersaturation at three different levels of temperature, i.e. 288, 298, and 308 K. As mentioned in the section of supersaturation effect, the best values of $\bar{g}$ and δ based on the total absolute deviation must be found before calculating the theoretical induction period from Eq. (8). It is found that the total absolute deviation have a smallest value for $\bar{g} = 2$ and $\delta = 67.9$ mJ/m^2 at 288 K

Table 2
A comparison of the calculated $t_{ind,the}$ and experimental $t_{ind,exp}$ obtained by using Eq. (8) at $\bar{g}=2$, $\delta=68.4$ mJ/m^2, and $T=298$ K

$[CaCl_2]=[Na_2CO_3]$ (kgmol/m^3)	S_a (dimensionless)	$\frac{3\eta}{4kT}$ (s/m^3)	$n^{-1}\exp[-\bar{g}\ln S_a+\delta/kT$ $(4\pi)^{1/3}(3\bar{g}V_m)^{2/3}]$ $(=1/n_{\bar{g}})$ (m^3/no.)	$\frac{32\pi V_m^2\delta^3}{3\bar{g}(kT\ln S_a)^3}-1$ $(=g_c/\bar{g}-1)$ (dimensionless)	$t_{ind,the}$ (s)	$t_{ind,exp}$ (s)
0.00075	3.96	1.823E+17	5.841E − 17	110.0	1171	1250
0.00100	4.37	1.823E+17	3.598E − 17	89.0	584	550
0.00150	5.06	1.823E+17	1.789E − 17	67.0	219	202
0.00200	5.79	1.823E+17	1.025E − 17	52.5	98	94
0.00250	6.41	1.823E+17	6.689E − 18	44.0	54	78
0.00300	6.90	1.823E+17	4.810E − 18	39.0	34	45
0.00350	7.37	1.823E+17	3.614E − 18	35.5	23	36
0.00400	7.88	1.823E+17	2.766E − 18	32.0	16	24
0.00425	8.11	1.823E+17	2.322E − 18	30.5	13	13

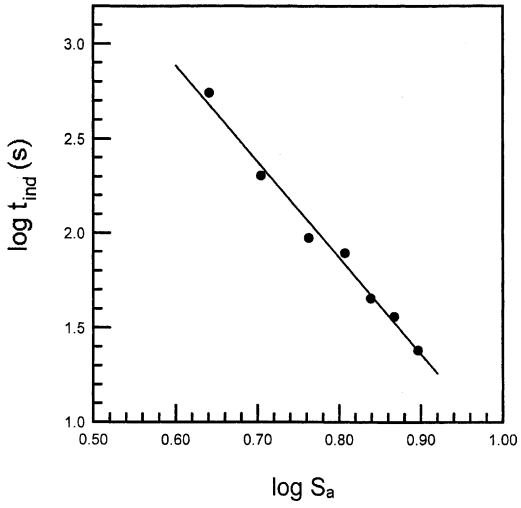

Fig. 5. A plot of Eq. (12) for calculation of nucleation order at 298 K.

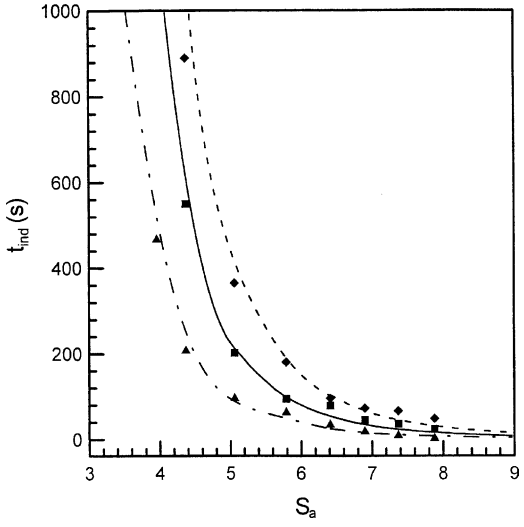

Fig. 6. Induction period as a function of supersaturation at different levels of solution temperature: ♦ experimental point for $T=288$ K; ■ experimental point for $T=298$ K; ▲ experimental point for $T=308$ K; - - - - theoretical curve at $T=288$ K for $\bar{g}=2$ and $\delta=67.9$ mJ/m^2; —— theoretical curve at $T=298$ K for $\bar{g}=2$ and $\delta=68.4$ mJ/m^2; –·– theoretical curve at $T=308$ K for $\bar{g}=2$ and $\delta=68.4$ mJ/m^2.

and $\bar{g}=2$ and $\delta=68.4$ mJ/m^2 at 308 K. Therefore, the most proper values of $\bar{g}$ and δ for calculating induction period are 2 and 67.9 mJ/m^2, respectively, for $T=288$ K, and 2 and 68.4 mJ/m^2, respectively, for $T=298$ and 308 K. The experimental results show that the induction periods increase with decreasing temperature at constant supersaturation and the experimental data are in a good agreement with the calculated values. The results imply that the dimer is a dominant size of clusters existing in the supersaturated solution to form nuclei when the solution temperature and supersaturation changes in a narrow range. Besides, the results also indicate that the interfacial tension δ does not vary within the range studied. Ginde and Myerson (1992) employed interferometric techniques to show that the average number of monomers in a cluster depends on the temperature and supersaturation of solution and varies with time after the creation of supersaturation. Estimated from diffusion data, the average number of monomers in a cluster is 1.92 for glycine at $S_a=1.14$, 1.23 for potassium chloride at $S_a=1.04$, 1.10 for sodium chloride at $S_a=1.03$, and 2.2 for potassium sulfate at $S_a=1.03$. The results indicate that there are very few large clusters in solution, and monomer and dimer are dominating in a supersaturated solution. Further, the induction periods calculated from Eq. (8) for $\bar{g}=2$ and $S_a=5.06$ at $T=288$, 298 and 308 K are summarized in Table 3 for further analysis. Table 3 shows that the decrease in induction period at higher solution temperature is caused by the higher diffusivity of clusters, higher initial coagulation concentration of clusters, and smaller critical nuclei size; among the three factors the coagulation concentration is the most significant one. Moreover, the present analysis reveals that the interfacial tension of $CaCO_3$ is not affected greatly by changing temperature from 288 to 308 K. This finding is in contradiction with the general conclusions obtained by using the

Table 3
The calculated results of Eq. (8) at $[CaCl_2] = [Na_2CO_3] = 0.0015$ kgmol/m^3 and $S_a = 5.06$ for different operating temperatures

Temperature (K)	δ (mJ/m^2)	$\frac{3\eta}{4kT}$ (s/m^3)	$n^{-1}\exp[-\bar{g}\ln S_a + \delta/kT$ $(4\pi)^{1/3}(3\bar{g}V_m)^{2/3}]$ $(=1/n_{\bar{g}})$ (m^3/no.)	$\frac{32\pi V_m^2\delta^3}{3\bar{g}(kT\ln S_a)^3} - 1$ $(=g_c/\bar{g} - 1)$ (dimensionless)	$t_{ind,the}$ (s)	$t_{ind,exp}$ (s)
288	67.9	1.886E+17	2.957E − 17	71.0	396	365
298	68.4	1.823E+17	1.789E − 17	67.0	219	202
308	68.4	1.764E+17	9.398E − 18	60.0	100	98

Table 4
The experimental t_{ind} and its corresponding theoretical values of δ obtained by using Eq. (8) at $\bar{g} = 2$ and $T = 298$ K for various values of $[Mg^{2+}]$ at five different reagent concentrations of $CaCl_2$ and Na_2CO_3

$[CaCl_2] = [Na_2CO_3]$ (kgmol/m^3)														
0.0015			0.0025			0.0035			0.0040			0.0045[a]		
$[Mg^{2+}]$ (kgmol/m^3)	$t_{ind,exp}$ (s)	δ (mJ/m^2)	$[Mg^{2+}]$ (kgmol/m^3)	$t_{ind,exp}$ (s)	δ (mJ/m^2)	$[Mg^{2+}]$ (kgmol/m^3)	$t_{ind,exp}$ (s)	δ (mJ/m^2)	$[Mg^{2+}]$ (kgmol/m^3)	$t_{ind,exp}$ (s)	δ (mJ/m^2)	$[Mg^{2+}]$ (kgmol/m^3)	$t_{ind,exp}$ (s)	δ (mJ/m^2)
0	202	68.2	0	78	69.5	0	36	69.7	0	24	69.6	0	—	—
0.0003	210	68.3	0.0005	90	69.9	0.0007	54	70.9	0.0008	36	70.8	0.0009	14	68.9
0.0006	250	68.8	0.0010	145	71.3	0.0014	70	71.7	0.0016	54	72.0	0.0018	40	72.0
0.0009	345	69.8	0.0015	180	72.0	0.0021	96	72.7	0.0024	84	73.3	0.0027	70	73.8
0.0012	375	70.0	0.0020	240	72.9	0.0028	150	74.0	0.0032	132	74.7	0.0041	140	75.8
0.0015	510	71.0	0.0025	360	74.1	0.0035	225	75.2	0.0040	210	76.1	—	—	—

[a]Data reported by Söhnel and Mullin (1982).

classical nucleation theory. For example, by analyzing the experimental data of t_{ind}-S_a for potash alum at different levels of temperature Mullin and Žáček (1981) concluded that the lower interfacial tension at higher temperature (3.14 mJ/m^2 at 288 K vs. 2.03 mJ/m^2 at 308 K) under a constant supersaturation is responsible for the shorter induction period. A question remains whether the two systems, i.e., readily soluble compound versus sparingly soluble compound, behave differently.

4.3. Effect of additive on induction period

The experimental values of induction period obtained at various molar concentration of Mg^{2+} are summarized in Table 4 for five different reagent concentrations of $CaCl_2$ and Na_2CO_3. The data of t_{ind} for 0.0045 kgmol/m^3 are reported by Söhnel and Mullin (1982). Table 4 shows that the presence of Mg^{2+} prolongs the induction period, which also increases with increasing $[Mg^{2+}]$ for all levels of reagent concentration of $CaCl_2$ and Na_2CO_3. Söhnel and Mullin (1982) found that the presence of Mn^{2+} or Mg^{2+} in aqueous $CaCl_2$–Na_2CO_3 solution lengthens the induction period of $CaCO_3$. They concluded that the increase in t_{ind} is due to an increase in the crystal-solution interfacial tension caused by the additives. Therefore, we try to express the interfacial tensions as a function of magnesium ion concentration. Let $\bar{g} = 2$ and substitute this value together with the experimental t_{ind} obtained at various concentrations of Mg^{2+} into Eq. (8), the interfacial tension is calculated. The calculated values of interfacial tension, δ, are also listed in Table 4 and plotted against $[Mg^{2+}]$ as shown in Fig. 7. It appears that the interfacial tension of $CaCO_3$ can be expressed as a linear function of magnesium ion concentration as the following correlation:

$$\delta = 2028.4 \times [Mg^{2+}] + 68.4. \quad (13)$$

Eq. (13) shows that the interfacial tension increases with increasing magnesium ion concentration in solutions. Therefore, the effect of Mg^{2+} on the induction period of $CaCO_3$ can be explained by an increase in the interfacial tension of $CaCO_3$. The larger interfacial tension results in a smaller coagulation concentration of clusters and a larger critical size of nuclei and thus a longer induction period.

4.4. Effect of seed crystals on induction period

Fig. 8 shows the experimental and theoretical data of induction period in the presence of seed crystals for different values of supersaturation at 298 K. The corresponding results obtained in the unseeded case are also shown for comparison. The experimental results indicate that the induction periods of seeded case are shorter than those obtained in the unseeded case for all cases. In the theoretical calculation we used the same values of $\bar{g}$ and δ as in the unseeded case. Therefore, the theoretical curve of induction period of seeded case is plotted by substituting $\bar{g} = 2$,

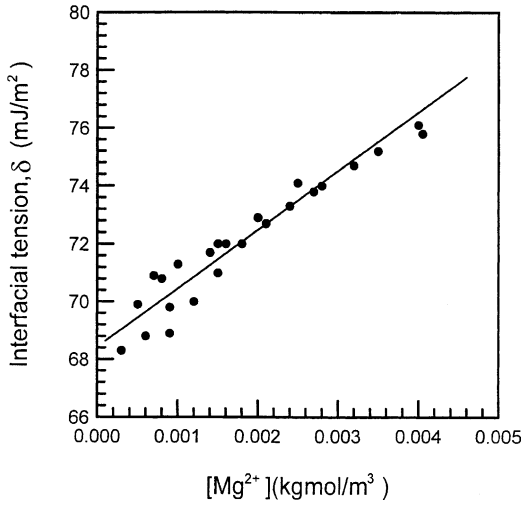

Fig. 7. The interfacial tension as a function of $[Mg^{2+}]$ at 298 K.

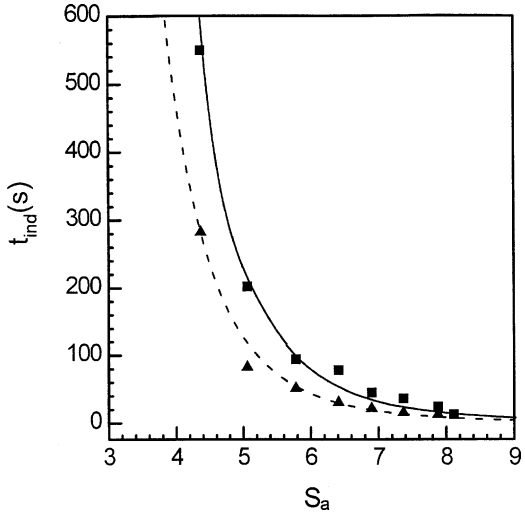

Fig. 8. Induction period as a function of S_a at 298 K for unseeded and seeded cases: ■ experimental point for unseeded case; ▲ experimental point for seeded case; —— theoretical curve for unseeded case: $\bar{g} = 2$ and $\delta = 68.4$ mJ/m^2; - - - - theoretical curve for seeded case: $\bar{g} = 2$, $\delta = 68.4$ mJ/m^2, and $d = 3.2 \times 10^{-10}$ m.

$\delta = 68.4$ mJ/m^2 and a given value of d into Eq. (11). By calculating the total absolute deviations, ε, between the experimental and theoretical induction periods, it is found that the ε have a smallest value at $d = 3.2 \times 10^{-10}$ m. It can be seen that the theoretical curve plotted by setting $\bar{g} = 2$, $\delta = 68.4$ mJ/m^2, and $d = 3.2 \times 10^{-10}$ m are close to the experimental points as shown in Fig. 8. The present analysis reveals that the decrease in induction period is attributed to the higher coagulation concentration of clusters formed in the region near the seed crystals. The higher coagulation concentration of clusters results from the van der Waals attractive force between the clusters and seed crystals. Moreover, the analysis also implies that the nucleation occurs at a distance 3.2×10^{-10} m from the surface of seed crystals. The distance is about 1.5 radius of $CaCO_3$ monomer. The present result obtained in sparingly soluble system is similar to that obtained by Qian and Botsaris (1997) in the soluble KCl system. They predicted that the nucleation occurs at a distance 4.92×10^{-10} m from the surface of seed crystals. The distance is about 2 radius of KCl monomer. Recently, Kuznetsov et al., (1996) has also found that at the vicinity of a crystal has a relatively high supersaturation than bulk solution in their study of protein precipitation by using the atomic force microscopy. The results imply the high probability of nucleation occurrence near the surface of seed crystals. Thus, the van der Waals attractive force between the clusters and seed crystals may responsible for the catastrophic secondary nucleation.

5. Conclusion

The effects of supersaturation, temperature, and the presence of Mg^{2+} and seed crystals on the induction period of $CaCO_3$ are studied experimentally and theoretically. In experimental, the results show that the induction period increases with a decrease in supersaturation and temperature. The presence of Mg^{2+} in solution prolongs the induction period. On the other hand, addition of seed crystals in solution reduces the induction period. The theoretical analysis shows that the decrease in induction period at higher supersaturation is mainly caused by the higher coagulation concentration of clusters and the smaller critical size of nuclei. The decrease in induction period at higher solution temperature is caused by the higher diffusivity of clusters, higher initial coagulation concentration of clusters, and smaller critical size of nuclei. For the presence of Mg^{2+} in solution the interfacial tension of $CaCO_3$ increases with increasing concentration of magnesium ion. The increase in induction period in the presence of Mg^{2+} is mainly caused by a larger interfacial tension. Finally, the effect of seed crystals on the induction period is caused by the higher coagulation concentration of clusters in the region near the seed crystal, resulting from the van der Waals attractive force between the clusters and seeds. This study indicates that the present cluster coagulation model is suitable for describing the effect of various operating variables on the induction period of $CaCO_3$.

Notation

A	Hamaker constant, J
C	concentration, kgmol/m^3
d	distance from the crystal surface, m
D	diffusivity of clusters, m^2/s
$\Delta G_{\bar{g}}$	excess free energy of the formation of a $\bar{g}$-mer cluster, J

g_c	number of monomer in a critical nuclei
$\bar{g}$	the dominating size of clusters in the solution
k	Boltzmann constant, J/K
n_o	initial number concentration of monomers in liquid phase, No./m^3
n_1	number concentration of monomers in liquid phase, No./m^3
$n_{\bar{g}}$	number concentration of $\bar{g}$-mer in liquid phase, No./m^3
r_1	radius of a spherical monomer, m
S_a	supersaturation
t_{ind}	induction period, s
T	temperature, K
V_m	volume of monomer, m^3

Greek letters

γ	mean activity coefficient
δ	interfacial tension of the crystal or cluster, mJ/m^2
ε	total absolute deviation of induction period
η	viscosity of the liquid, Pa s

Acknowledgements

This study is supported by the National Science Council of the Republic of China.

References

Bergström, L. (1997). Hamaker constants of inorganic materials. *Advances in Colloid and Interface Science*, *70*, 125–169.

Bromley, L. A. (1973). Thermodynamic properties of strong electrolytes in aqueous solutions. *AIChE*, *19*, 313–320.

Carosso, P. A., & Pelizzetti, E. (1984). A stopped-flow technique in fast precipitation kinetics—the case of barium sulphate. *Journal of Crystal Growth*, *68*, 532–536.

Chien, W. C., Tai, C. Y., & Hsu, J. P. (1999). The induction period of the $CaCl_2$–Na_2CO_3 system: Theory and experimental. *Journal of Chemical Physics*, *111*, 2657–2664.

Ginde, R. M., & Myerson, A. S. (1992). Cluster size estimation in binary supersaturated solutions. *Journal of Crystal Growth*, *116*, 41–45.

Glasner, A., & Tassa, M. (1972). The thermal effects of nucleation and crystallization of KBr solutions. *Journal of Crystal Growth*, *13/14*, 441–444.

Gómez-Morales, J., Torrent-Burgués, J., & Rodríguez-Clemente, R. (1996). Nucleation of calcium carbonate at different initial pH conditions. *Journal of Crystal Growth*, *169*, 331–338.

Kibalczyc, W., & Bondarczuk, K. (1985). Light scattering study of calcium phosphate precipitation. *Journal of Crystal Growth*, *71*, 751–756.

Kibalczyc, W., & Zielenkiewicz, A. (1987). Calorimetric investigations of calcium phosphate precipitation. *Journal of Crystal Growth*, *82*, 733–736.

Koutsoukos, P. G., & Kontoyannis, C. G. (1984). Precipitation of calcium carbonate in aqueous solutions. *Journal of Chemical Society Faraday Transaction I*, *80*, 1181–1192.

Kubota, N., Kawakami, T., & Tadaki, T. (1986). Calculation of supercooling temperature for primary nucleation of potassium nitrate from aqueous solution by the two-kind active site model. *Journal of Crystal Growth*, *74*, 259–274.

Kuznetsov, Y. G., Malkin, A. J., Glantz, W., & Mcpherson, A. (1996). In situ atomic force microscopy studies of protein and virus crystal growth mechanisms. *Journal of Crystal Growth*, *168*, 63–73.

Mullin, J. W. (1993). *Crystallization* (3rd ed.). Oxford: Butterworth-Hienemann (Chapter 5).

Mullin, J. W., & Žáček, S. (1981). The precipitation of potassium aluminium sulphate from aqueous solution. *Journal of Crystal Growth*, *53*, 515–518.

Nielsen, A. E. (1964). *Kinetics of precipitation*. Oxford: Pergamon Press.

Packter, A. J. (1974). The precipitation of calcium sulphate dihydrate from aqueous solution. *Journal of Crystal Growth*, *21*, 191–194.

Pokrovsky, O. S. (1998). Precipitation of calcium and magnesium carbonates from homogeneous supersaturated solutions. *Journal of Crystal Growth*, *186*, 233–239.

Qian, R. Y., & Botsaris, G. D. (1997). A new mechanism for nuclei formation in suspension crystallizers: The role of interparticle forces. *Chemical Engineering Science*, *52*, 3429–3440.

Söhnel, O., & Garside, J. (1992). *Precipitation: Basic principles and industrial applications*. Oxford: Butterworth-Heinemann (Chapter 3).

Söhnel, O., & Mullin, J. W. (1978). A method for the determination of precipitation induction periods. *Journal of Crystal Growth*, *44*, 377–382.

Söhnel, O., & Mullin, J. W. (1982). Precipitation of calcium carbonate. *Journal of Crystal Growth*, *60*, 239–250.

Söhnel, O., & Mullin, J. W. (1988). Interpretation of crystallization induction periods. *Journal of Colloidal and Interface Science*, *123*, 43–50.

Sonntag, H., & Strenge, H. (1987). *Coagulation kinetics and structure formation*. New York: Plenum Press (Chapter 3).

Tai, C. Y., & Chien, W. C. (2001). Effects of operating variables on the induction period of $CaCl_2$–Na_2CO_3 system. Paper presented at 13th international conference on crystal growth, Kyotanabe, Kyoto, Japan, 2001.

Verdoes, D., Kashchiev, D., & van Rosmalen, G. M. (1992). Determination of nucleation and growth rates from induction times in seeded and unseeded precipitation of calcium carbonate. *Journal of Crystal Growth*, *118*, 401–413.

Wakita, M. I. H., & Masuda, I. (1983). Analyses of precipitation processes of bis(dimethylglyoximato)Ni(II) and related complexes. *Journal of Crystal Growth*, *61*, 377–382.